GMR
The Original

PHYSIOCHEMICAL PROPERTIES AND ANTIMICROBIAL EFFICACY OF NOVEL STARCH/PVA/CUO ELECTROSPUN NANOSCAFFOLDS FROM *SARGASSUM MUTICUM* (BROWN MARINE MACROALGAE) EXTRACT

Akshayaa Paramasivan[1], Sinega NS[2], Anand KH[3], Rajalakshmi Anbalagan[4]*, Sattanathan Govindharajan[5]*

[1]Saveetha Medical College & Hospital (SMCH), Saveetha Institute of Medical and Technical Sciences (SIMATS), Thandalam, Chennai, Tamil Nadu 602105, India. akshivan1965@gmail.com
[2]Department of Pathology, Saveetha Medical College and Hospital, Saveetha Institute of Medical And Technical Sciences (SIMATS), Thandalam, Chennai-602105, Tamil Nadu, India. Email: sinegasivasamy95@gmail.com; ORCID: https://orcid.org/0009-0005-1788-5401.
[3]Department of ENT, Saveetha Medical College and Hospital, Saveetha Institute of Medical And Technical Sciences (SIMATS), Thandalam, Chennai-602105, Tamil Nadu, India. Email: anandkh91@gmail.com. ORCID: https://orcid.org/0000-0001-8496-5675.
[4]Department of Biochemistry, A.D.M. college for Women (Autonomous), Nagapattinam, Tamil Naud-611001, India. Email: abioraji@gmail.com; ORCID: https://orcid.org/ 0000-0003-3723-9923.
[5]Department of Pathology, Saveetha Medical College and Hospital, Saveetha Institute of Medical And Technical Sciences (SIMATS), Thandalam, Chennai-602105, Tamil Nadu, India. Email: sattanathanphd@gmail.com

*Correspondence: abioraji@gmail.com (R.A.), sattanathanphd@gmail.com (S.G.)

ABSTRACT
This study explores the green synthesis of copper oxide nanoparticles (CuO NPs) using *Sargassum muticum* extract and their incorporation into starch/polyvinyl alcohol (PVA) electrospun nanoscaffolds for enhanced antimicrobial applications. The phytochemical-rich algal extract facilitated the eco-friendly reduction of Cu^{2+} ions, yielding stable CuO NPs, which were characterized using UV-Vis spectroscopy, Fourier-transform infrared spectroscopy (FTIR), X-ray diffraction (XRD), Scanning electron microscopy (SEM), Thermogravimetric analysis (TGA), and zeta potential analysis. UV-Vis spectroscopy confirmed nanoparticle formation via a distinct surface plasmon resonance (SPR) peak at 270 nm, while FTIR revealed functional groups involved in stabilization. XRD confirmed the monoclinic crystalline structure of CuO NPs, and SEM demonstrated uniform dispersion within nanofibers. The starch/PVA scaffolds exhibited high porosity and thermal stability, with TGA indicating enhanced degradation resistance. Antimicrobial assays revealed significant inhibitory effects against bacterial (*Escherichia coli*, *Staphylococcus aureus*) and fungal (*Aspergillus niger*, *Penicillium* spp.) pathogens, with nanoscaffolds outperforming pure CuO NPs and algal extract. These findings highlight the potential of algae-mediated CuO NPs in developing biocompatible, antimicrobial nanoscaffolds for wound healing and tissue engineering, offering a sustainable alternative to conventional antimicrobial agents.

KEYWORDS: *Sargassum muticum*, Green synthesis, CuO NPs, Starch/PVA nanoscaffolds, Antimicrobial activity.

1. INTRODUCTION

The convergence of nanotechnology with marine biotechnology has opened new avenues in the synthesis of eco-friendly, biologically potent nanomaterials [1]. Among these, marine macroalgae—commonly known as seaweeds—have emerged as a sustainable source of biomolecules capable of reducing metal ions into stable nanoparticles [2]. Owing to their rich phytochemical reservoir, including phenolics, flavonoids, and sulfated polysaccharides, these marine organisms serve not only as reducing agents but also as capping and stabilizing entities during nanoparticle synthesis [3]. This green synthesis approach significantly contrasts with conventional physical and chemical methods, which often involve toxic solvents, high energy demands, and hazardous by-products, thus making marine algae-based methods more biocompatible and environmentally benign [4].

Sargassum muticum (S. muticum), a brown marine macroalga prevalent along the southeastern coast of India, including the intertidal zones of Rameswaram, is particularly rich in bioactive constituents such as fucoidans, alginates, terpenoids, and polyphenols [5]. These compounds exhibit a wide spectrum of therapeutic properties including antioxidant, antimicrobial, and anti-inflammatory activities [6]. The abundance and easy accessibility of *S. muticum* make it an ideal candidate for biotechnological applications, particularly in the realm of green nanomaterial synthesis [7]. Its role as a bioresource in the production of metal oxide nanoparticles, such as copper oxide nanoparticles (CuO NPs), is garnering increasing interest in recent years [8].

CuO NPs have drawn considerable attention owing to their unique physicochemical properties, including a narrow band gap, high surface area, and potent antimicrobial and catalytic activities [9]. CuO is a p-type semiconductor with applications ranging from sensors, supercapacitors, and photocatalysis to biomedical uses such as wound healing and drug delivery [10]. Notably, CuO NPs have demonstrated superior antimicrobial and antifungal properties due to their ability to generate reactive oxygen species (ROS), disrupt microbial cell membranes, and bind to cellular enzymes, thus impairing microbial function [11]. These attributes make CuO NPs an attractive component in the design of novel biomedical materials [12].

One of the most promising applications of CuO NPs lies in their integration into nanofibrous scaffolds for tissue engineering and wound healing [13]. Electrospinning is a well-established technique that enables the fabrication of continuous nanofibers with high surface-area-to-volume ratios and tunable porosity—properties that closely mimic the natural extracellular matrix (ECM) [14]. When combined with biopolymers such as starch and polyvinyl alcohol (PVA), the electrospun mats can serve as efficient platforms for controlled release and localized delivery of therapeutic agents [15]. Starch, being biodegradable and biocompatible, acts as a reinforcing matrix, while PVA provides mechanical stability and facilitates the electrospinning process [16]. Embedding CuO NPs into starch/PVA nanofibers enhances the functional performance of these scaffolds, making them suitable for biomedical applications [17].

The integration of green-synthesized CuO NPs into a biopolymer-based electrospun scaffold not only improves the mechanical and thermal properties of the matrix but also endows it with antimicrobial and wound-healing potential [18]. The uniform distribution of nanoparticles within the fiber matrix is crucial for sustained release, optimal interaction with the biological environment, and minimizing toxicity [19]. Furthermore, such hybrid systems offer an eco-friendly alternative to synthetic drugs and conventional wound dressings, aligning with the growing demand for sustainable biomedical solutions [20].

Despite the increasing number of studies exploring nanoparticle-loaded electrospun scaffolds, the synthesis of CuO NPs using *S. muticum* extract and their incorporation into starch/PVA matrices remains underexplored [17]. The current study seeks to address this gap by employing ultrasonic-assisted extraction to obtain phytochemically rich extracts from *S. muticum*, followed by the green synthesis of CuO NPs [21]. The synthesized nanoparticles are subsequently embedded into starch/PVA electrospun nanofibers to develop multifunctional scaffolds with potential applications in wound healing and tissue engineering [22].

The study emphasizes a comprehensive characterization of both the synthesized CuO NPs and the electrospun scaffolds using a suite of analytical techniques [23]. UV-Vis spectroscopy is utilized to confirm nanoparticle formation via surface plasmon resonance (SPR) [24], while Fourier transform infrared (FTIR) spectroscopy provides insights into the functional groups involved in nanoparticle stabilization and scaffold matrix interactions [25]. X-ray diffraction (XRD) analysis elucidates the crystalline nature and phase identity of the CuO NPs and nanofibers [26]. Scanning electron microscopy (SEM) is employed to observe morphological features, fiber uniformity, and nanoparticle dispersion within the scaffolds [27]. Thermogravimetric analysis (TGA) further assesses the thermal stability and decomposition profiles of the composite materials, whereas zeta potential and particle size distribution measurements offer information on colloidal stability and aggregation tendencies of the nanoparticles.

By combining marine-derived phytochemicals with copper oxide nanotechnology and electrospinning methodologies, this research bridges the gap between marine bioprospecting and biomedical engineering. It presents a novel, green, and scalable route for developing functional biomaterials tailored for wound healing applications. Furthermore, the study contributes to the growing body of literature advocating for the sustainable synthesis and biomedical application of nanomaterials derived from renewable marine resources.

The present research explores the untapped potential of *S. muticum* for the biosynthesis of CuO NPs and their successful integration into starch/PVA-based electrospun nanofibrous scaffolds. The developed materials are characterized extensively for their structural, chemical, and thermal properties, setting the foundation for future applications in wound healing and tissue regeneration. This multidisciplinary approach underscores the synergy between natural resources, nanotechnology, and material science, offering promising prospects for the next generation of eco-friendly biomedical devices.

2. MATERIALS AND METHODS

2.1. Collection and preparation of marine macroalgae

Fresh samples of *S. muticum* were manually gathered from the intertidal regions surrounding Rameswaram and transported to the lab under chilled conditions. The algal material was initially rinsed with tap water to eliminate soil particles, debris, and surface-dwelling organisms. This was followed by several washes with distilled water to ensure thorough cleansing. The cleaned algae were then chopped into smaller sections and left to dry naturally in a shaded, well-aerated environment at room temperature for approximately 14 days. Once fully dried, the samples were pulverized into fine powder using a mechanical grinder and preserved in airtight containers at ambient conditions until further processing.

2.2. Ultrasonic-assisted extraction of bioactive compounds

To isolate phytochemicals from *S. muticum*, 2 grams of the dried powdered material were mixed with 50 mL of Milli-Q water and exposed to ultrasonic-assisted extraction using a LABQUEST ultrasonic bath (Borosil; Serial No. 941032329018) at 60°C for 45 minutes. The cavitation generated during sonication enhanced the release of bioactive molecules. The mixture was then passed through Whatman No. 1 filter paper under sterile settings to yield a clarified extract. The filtered liquid was stored at 10°C for immediate use and subsequently lyophilized to produce a stable dry powder suitable for extended storage and downstream applications [28].

2.3. Green synthesis of CuO NPs

The synthesis of CuO NPs involved the reaction of 50 mL of 0.1 M $CuSO_4 \cdot 5H_2O$ solution with 10 mL of *S. muticum* extract, which was prepared by dissolving 10 mg of the lyophilized powder in 10 mL of Milli-Q water, maintaining a 5:1 volumetric ratio. This blend was continuously stirred at 650 rpm and maintained at 60°C for 2 hours. A visual color change from blue to bluish-green signaled the formation of CuO NPs through the reduction of copper ions. The resultant product was centrifuged and washed three times with double-distilled water to remove residual plant components and excess reagents. The purified nanoparticles were freeze-dried over 48 hours and stored in a desiccator for future characterization and application in nanofiber scaffolds [29].

2.4. Electrospinning of CuO-embedded starch/PVA nanofibrous scaffolds

To develop the composite nanofibers, a 15% (w/w) solution of PVA was created by dissolving the polymer in Milli-Q water under constant agitation until fully dissolved. Subsequently, 100 mg each of starch and CuO NPs were added to the PVA solution, followed by continuous stirring at 50°C for 2.5 hours to ensure even dispersion. The blend was loaded into a syringe fitted with a stainless steel needle (inner diameter 0.84 mm) and placed in the HOLMARC HO-NFES-040 electrospinning unit. The electrospinning conditions were optimized as follows: applied voltage of 11.5 kV, a 12.3 cm gap between the needle and collector, and a controlled flow rate of 0.4 mL/h. The process was performed at room temperature over 6–8 hours to form nanofibrous mats, which were then peeled off and preserved in a desiccator for further study [30, 31].

2.5. Physicochemical characterization of nanoparticles and scaffolds

2.5.1. UV-vis spectroscopy

The UV-Vis spectral analysis of the CuO NPs and algal extract was conducted using a VIS SPEC V-730 spectrophotometer within the 200–800 nm wavelength range. Deionized water was used as a blank. Characteristic SPR bands were observed, confirming nanoparticle synthesis [32, 33].

2.5.2. FTIR Spectroscopy analysis

FTIR spectra were recorded using a PerkinElmer Spectrum Two device in ATR mode. Spectral data for both CuO NPs and CuO-loaded scaffolds were collected between 4000 and 400 cm^{-1}, using a resolution of 4 cm^{-1} and 64 scans per sample. Peaks corresponding to hydroxyl, phenolic, carbonyl, and metal-oxygen bonds were identified [34, 35].

2.5.3. XRD analysis

XRD was used to analyze the crystalline nature and phase identity of CuO NPs and nanocomposite scaffolds via a Bruker D8 Advance system using CuKα radiation (λ = 1.5406 Å) at 40 kV and 40 mA. Data were recorded over a 2θ range from 5° to 90° with a 0.029649° step size. Peaks were matched against JCPDS database patterns to confirm CuO presence [36, 37].

2.5.4. SEM analysis

The morphological characteristics of the nanoparticles and nanofiber matrices were observed using a JEOL JSM-IT800 NANO SEM. Gold sputter coating was applied to enhance conductivity. SEM images were analyzed to evaluate fiber diameter, particle dispersion, and surface texture [38, 39].

2.5.5. TGA

Thermal decomposition behavior and stability of the scaffolds were assessed with a PerkinElmer TGA 8000 under a nitrogen atmosphere. Approximately 5 mg of the sample was gradually heated from room temperature to 550°C at a rate of 15°C/min. The thermograms provided insights into moisture content, degradation temperatures, and residual mass [40, 41].

2.5.6. Zeta potential and particle size distribution

The hydrodynamic diameter and surface charge (zeta potential) of the CuO NPs were measured using a Malvern Zetasizer Ultra. Zeta potential values indicated colloidal dispersion stability; higher absolute values suggested increased electrostatic repulsion and better suspension stability [42, 43].

All experimental raw data and corresponding analysis results are available in the Mendeley Data repository under DOI: 10.17632/vf8822rd8j.1 for public access.

2.7. Antimicrobial activity analysis

The antibacterial and antifungal efficacy of *S. muticum* extract, CuO NPs, and starch/PVA electrospun nanoscaffolds (50 µg/mL each) was evaluated using the agar well diffusion assay. Test microorganisms included Gram-negative (*Escherichia coli*, *Klebsiella pneumoniae*, *Citrobacter koseri*) and Gram-positive (*Staphylococcus aureus*) bacteria, as well as fungal species (*Aspergillus niger*, *Penicillium* sp.). Bacterial cultures were adjusted to 0.5 McFarland standard (~1.5×10^8 CFU/mL) and swabbed onto Mueller-Hinton agar plates, while fungal spores were inoculated on Sabouraud dextrose agar. Wells (6 mm diameter) were loaded with 50 µL of each test sample. Ciprofloxacin (for bacteria) and voriconazole (for fungi) served as positive controls. After a 30-minute diffusion period, bacterial plates were incubated at 37°C for 24 hours, and fungal plates at 28°C for 48 hours. Antimicrobial activity was quantified by measuring the diameter (mm) of the inhibition zones. All tests were performed in triplicate to ensure reproducibility [44-48].

2.8. Statistical analysis

All data analyses were carried out using SPSS version 25.0 and GraphPad Prism version 9.0. Values were expressed as mean ± standard deviation (SD) from three separate trials. One-way ANOVA was conducted to assess differences between experimental groups, with post hoc Tukey's and Dunnett's tests applied where necessary. Statistical significance was accepted at $p < 0.05$. The Shapiro-Wilk test confirmed the normal distribution of datasets, and Pearson's correlation was used to determine the strength of associations between variables. All statistical interpretations were made with a 95% confidence level [49].

3. RESULTS AND DISCUSSION

3.1. UV–vis spectroscopy

The optical properties of the *S. muticum* extract and the synthesized CuO NPs were examined using a JASCO V-730 UV–Visible spectrophotometer. Spectral measurements were recorded over a wavelength range of 200–800 nm at 1 nm intervals (Fig. 1), using deionized water as the baseline reference. The *S. muticum* extract exhibited a broad absorption pattern typical of natural phytochemical constituents, such as flavonoids and polyphenols. In contrast, the CuO NPs demonstrated a sharp and distinct absorption peak centered at 270 nm, which corresponds to SPR—a characteristic phenomenon confirming the formation of metallic nanoparticles. The spectrophotometer parameters included a 1.0 nm bandwidth, a scan speed of 1000 nm/min, and continuous filter exchange for optimal signal resolution. The CuO NPs exhibited a maximum absorbance of 0.477617 at 270 nm, reinforcing successful nanoparticle synthesis and their unique optical response compared to the plant extract alone [50-54].

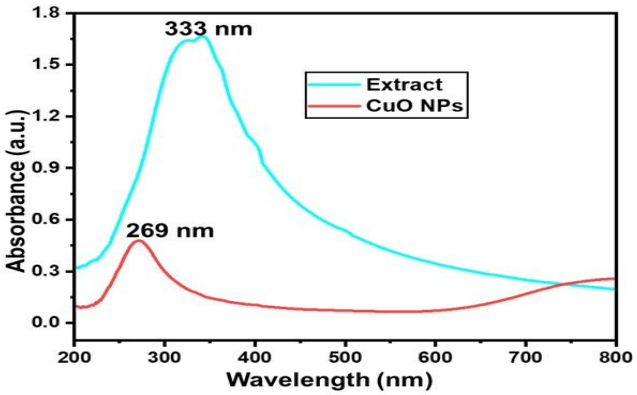

Fig. 1. UV–Visible spectral profiles of algal extract and CuO NPs.

3.2. FTIR spectroscopy analysis

The chemical functionalities and molecular interactions of CuO NPs and starch/PVA electrospun nanoscaffolds were characterized using FTIR spectroscopy (PerkinElmer Spectrum Two, ATR mode). Spectra were collected over the range of 4000–400 cm^{-1} with a resolution of 4 cm^{-1} and 64 scans per sample (Fig. 2). The CuO NP spectrum displayed a strong absorption peak at 3277.29 cm^{-1}, attributed to O–H stretching vibrations, indicating the presence of hydroxyl groups likely from capping phytochemicals. Additional peaks at 2700.50 cm^{-1} and 2500.00 cm^{-1} suggested C–H stretching and carbonyl functionalities, respectively. The FTIR spectrum of the starch/PVA nanoscaffolds showed characteristic peaks at 1500.00 cm^{-1}, corresponding to C=O stretching vibrations from carbonyl groups, and 840.00 cm^{-1}, representing C–O–C stretching in glycosidic bonds.

Importantly, the appearance of peaks below 1000 cm^{-1}—particularly near 600.00 cm^{-1}—was indicative of Cu–O bonding, validating the incorporation of CuO NPs into the polymer scaffold. These findings confirm the presence of essential functional groups such as phenolic, hydroxyl, and carbonyl moieties and demonstrate successful integration of CuO NPs within the nanocomposite matrix [55-59].

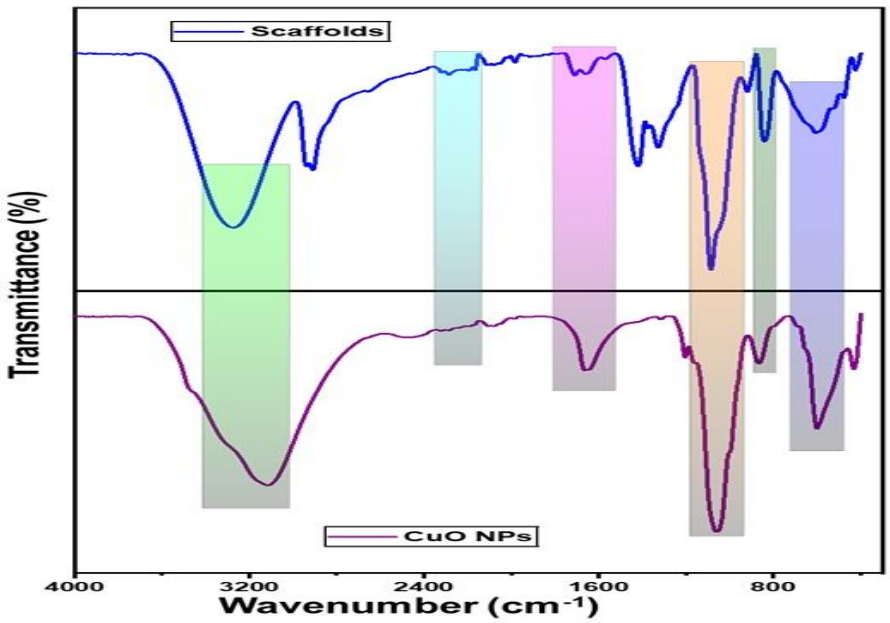

Fig. 2. FTIR spectra of CuO NPs and their incorporation into nanoscaffolds.

3.3. XRD analysis

XRD analysis was conducted to evaluate the crystalline nature of the synthesized CuO NPs and the starch/PVA electrospun scaffolds using a Bruker D8 Advance diffractometer equipped with CuKα radiation (λ = 1.5406 Å) operating at 40 kV and 40 mA. The diffraction patterns were recorded across a 2θ range of 5° to 90° with a step size of 0.029649° (Fig. 3). The CuO NPs exhibited sharp diffraction peaks at 32.745°, 35.297°, 38.307°, and 48.123°, corresponding to the (110), (002), (111), and (202) planes of monoclinic CuO, which matched standard JCPDS card no. 05-0661, confirming the high purity and crystalline nature of the nanoparticles. The starch/PVA scaffold exhibited broader peaks at 19.270°, 21.364°, and 23.525°, representing the semi-crystalline nature of the polymer blend. Additionally, peaks at 26.536° and 29.481° indicated interactions between the polymer matrix and the incorporated CuO NPs. Calculated d-spacing values (e.g., 2.732 Å for the (110) CuO plane) aligned well with reference values. The sharp peaks for CuO NPs contrasted with the broad polymer peaks, suggesting nanoscale crystallites embedded in an amorphous to semi-crystalline matrix. These results confirmed the structural integration of CuO NPs into the electrospun fibers and provided insights into crystallite dimensions and scaffold composition [60-64].

3.4. SEM analysis

The morphological characteristics of CuO NPs and the starch/PVA nanoscaffolds were analyzed (Fig. 4) using a JEOL JSM-IT800 NANO SEM system. Prior to imaging, the samples were sputter-coated with gold to improve electrical conductivity. SEM micrographs of the CuO NPs revealed predominantly spherical particles with slight morphological irregularities and agglomeration, which is common due to the high surface energy of nanoparticles. In contrast, the starch/PVA electrospun nanoscaffolds showed a well-organized fibrous architecture with interconnected porous structures. The fibers exhibited relatively uniform diameters. CuO NPs were visibly embedded on the fiber surfaces and within nodal junctions, indicating homogeneous dispersion within the polymer network. Surface texture analysis showed smooth fiber morphology, with occasional bead-like structures likely caused by fluctuations in electrospinning parameters such as polymer viscosity or applied voltage. The porous and nanofibrous morphology enhances the scaffolds' surface area, making them suitable for biomedical applications like tissue regeneration and drug delivery [65-71].

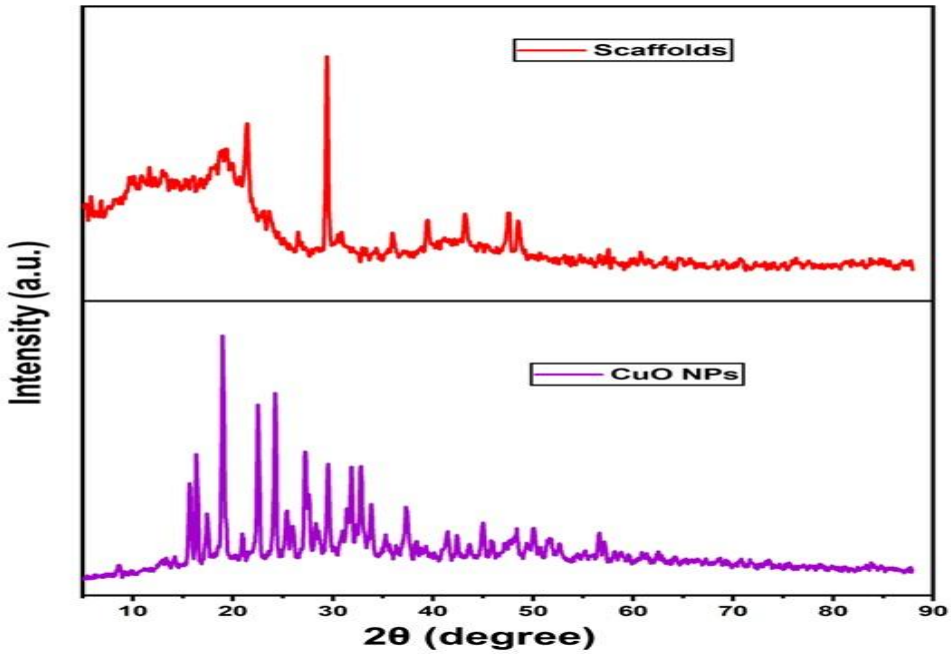

Fig. 3. XRD patterns of synthesized CuO NPs and CuO-loaded scaffolds.

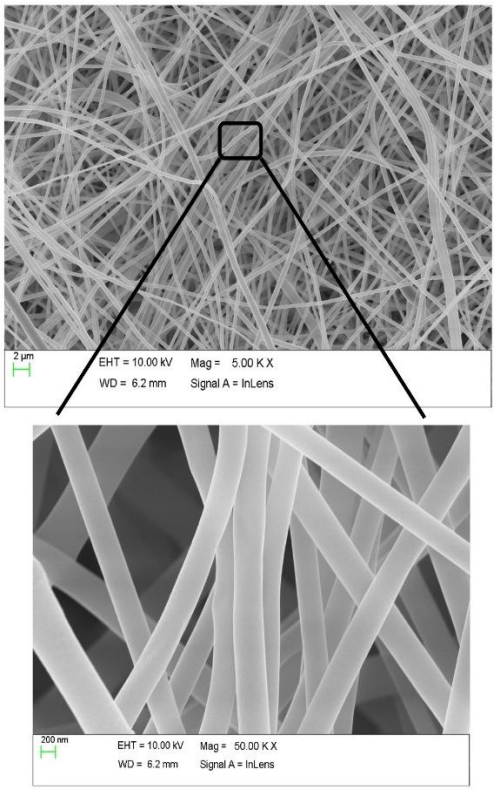

Fig. 4. SEM analysis of synthesized CuO NPs and CuO-loaded scaffolds.

3.5. TGA

The thermal stability and degradation profile of the starch/PVA electrospun nanoscaffolds were evaluated using a PerkinElmer TGA under nitrogen atmosphere. A sample weighing 1.187 mg was heated from room temperature to 550°C at a controlled rate (Fig. 5). The TGA curve exhibited a multi-step degradation pattern. The initial weight loss below 150°C was attributed to the evaporation of residual moisture. The major thermal decomposition onset occurred at 243.01°C, corresponding to the breakdown of the starch and PVA polymer chains. The maximum degradation rate was observed at 349.62°C, and degradation concluded around 393.07°C. The scaffold retained 51.881% of its original mass at the end of the heating cycle, suggesting the presence of thermally stable components such as inorganic CuO NPs and potential crosslinking between polymer chains. The significant weight loss between 200–400°C is characteristic of biopolymer degradation, while the high residual mass

indicates improved thermal resistance, which is crucial for biomedical applications requiring sterilization or heat treatment [72-76].

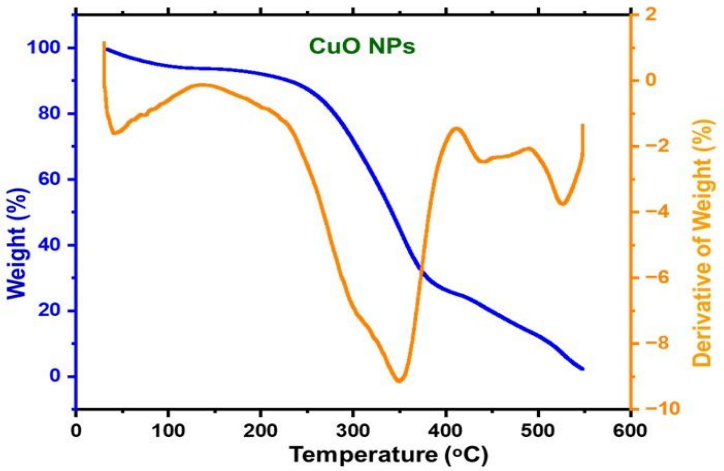

Fig. 5. Thermal degradation behavior of CuO-incorporated nanoscaffolds.

3.6. Zeta potential and particle size analysis

The colloidal behavior and hydrodynamic size of CuO NPs were investigated using dynamic light scattering (DLS) and zeta potential measurements with a Malvern Zetasizer Ultra. The intensity-weighted particle size distribution revealed an average hydrodynamic diameter (Z-average) of 92.1 nm (Fig. 6), indicating the formation of nanosized particles. The polydispersity index (PDI) was calculated to be 0.8444, suggesting moderate to high heterogeneity in particle sizes, potentially due to partial aggregation. Zeta potential analysis indicated a mean surface charge of −12.62 mV, with peak values recorded at −20.85 mV and −8.994 mV (Fig. 7). The negative zeta potential values suggest that the particles possess moderate colloidal stability due to electrostatic repulsion, which helps in minimizing agglomeration in aqueous suspensions. The conductivity (0.07909 mS/cm) and quality factor (5.109) further validated the reliability of the measurement. Collectively, these data confirm that the synthesized CuO NPs are moderately stable in suspension, with nanoscale dimensions and surface charge characteristics suitable for biological and environmental applications [77-79].

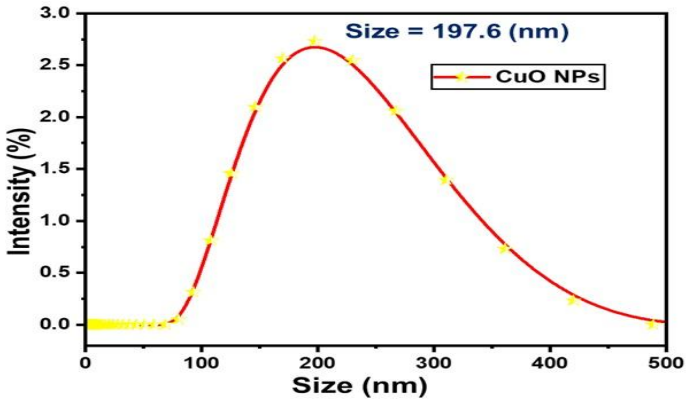

Fig.6. DLS particles size analysis of CuO NPs

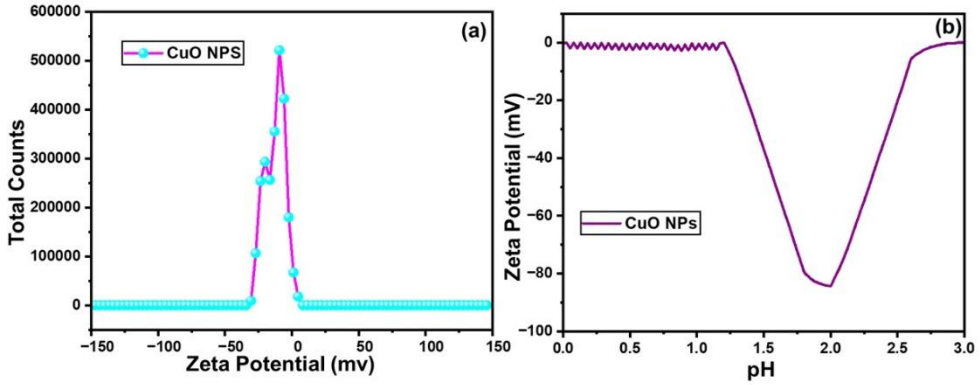

Fig.7. Zeta-potential analysis of CuO NPs

3.7. Antimicrobial activity analysis

The antimicrobial evaluation of *S. muticum* extract, CuO NPs, and starch/PVA electrospun nanoscaffolds at 50 µg/mL concentration demonstrated varying efficacy against pathogenic microorganisms (Table 1). The algal extract showed moderate antimicrobial activity, with inhibition zones ranging from 12±0.19 mm (*Staphylococcus aureus*) to 17±0.13 mm (*Penicillium* species) against bacterial and fungal strains, respectively. CuO NPs exhibited enhanced antibacterial effects (15±0.28 mm to 18±0.36 mm) and antifungal activity (19±0.24 mm to 20±0.32 mm), suggesting improved performance compared to the crude extract. Most notably, the starch/PVA nanoscaffolds embedded with CuO NPs displayed superior antimicrobial properties, with inhibition zones of 23±0.32 mm (*Escherichia coli*), 22±0.13 mm (*Klebsiella pneumoniae*), 20±0.26 mm (*S. aureus*), 22±0.12 mm (*Citrobacter koseri*), 25±0.28 mm (*Aspergillus niger*), and 24±0.12 mm (*Penicillium* species). While the nanoscaffolds demonstrated stronger antimicrobial effects than both the algal extract and standalone CuO NPs, their efficacy remained slightly below the positive controls ciprofloxacin (28-33 mm) and voriconazole (26-28 mm). These results indicate that the CuO NP-loaded nanoscaffolds offer synergistic antimicrobial benefits, making them promising candidates for biomedical applications requiring controlled antimicrobial release and enhanced biocompatibility. The study highlights the potential of marine algae-mediated nanoparticles in developing advanced antimicrobial materials [80-83].

Table 1: Antimicrobial activity of *S. muticum* extract, CuO NO, and starch/PVA electrospun nanoscaffolds at concentration of 50 µg/mL against various pathogenic organisms.

S. No	Organisms	Zone of inhibition (mm)				
		Ciprofloxacin (Antibiotic)	Voriconazole (Antifungal)	Algal Extract	CuO NPs	Nano-scaffolds
1.	*Escherichia coli*	33±0.58	-	15±0.28	18±0.36	23±0.32
2.	*Klebsiella pneumoniae*	30±0.14	-	13±0.12	16±0.34	22±0.13
3.	*Staphylococcus aureus*	28±0.32	-	12±0.19	15±0.15	20±0.26
4.	*Citrobacter koseri*	29±0.47	-	13±0.21	16±0.26	22±0.12
5.	*Aspergillus niger*	-	26±0.65	16±0.28	19±0.24	25±0.28
6.	*Penicillium* species	-	28±0.39	17±0.13	20±0.32	24±0.12

5. CONCLUSION

This study successfully demonstrated the green synthesis of CuO NPs using *S. muticum* extract and their incorporation into starch/PVA electrospun nanoscaffolds for enhanced antimicrobial applications. The phytochemical-rich algal extract facilitated the eco-friendly reduction of Cu^{2+} ions, yielding stable nanoparticles confirmed by UV-Vis spectroscopy (SPR peak at 270 nm), FTIR (functional group interactions), and XRD (monoclinic crystalline structure). SEM analysis revealed uniform nanoparticle dispersion within nanofibers, while TGA confirmed improved thermal stability of the composite scaffolds. Antimicrobial assays demonstrated significant inhibitory effects against bacterial (*Escherichia coli*, *Staphylococcus aureus*) and fungal (*Aspergillus niger*, *Penicillium* spp.) pathogens, with CuO-loaded nanoscaffolds outperforming both pure CuO NPs and algal extract. The synergistic antimicrobial action, combined with the scaffolds' biocompatibility and structural integrity, highlights their potential as advanced wound dressings or tissue engineering matrices. This research underscores the viability of marine algae-mediated green synthesis in developing sustainable, high-performance biomedical materials, offering a promising alternative to conventional antimicrobial agents. Future studies should focus on *in vivo* biocompatibility and long-term therapeutic efficacy to facilitate clinical translation.

Data Availability Statement: The full dataset of physiochemical characterization associated with this work is published in Mendeley Data [Dataset] Bioactive nanostructured platforms: Physicochemical assessment of starch scaffolds hybridized with Sargassum muticum-copper oxide nanoparticles (DOI: 10.17632/jrs2y2hp7v.2). **Disclosure:** The material characterization data and figures (e.g., UV, SEM, FTIR, XRD, TGA, Zeta Potential and particle sizer) presented here were generated from a common dataset and are being reused across multiple related studies on nanomaterials. All biological analyses and conclusions are original to each manuscript.

Conflicts of Interest: The authors declare no conflicts of interest.

REFERENCES

[1] Guo H, Liu Y, Wan T, Song D, Palanisamy CP, Geng J, Pei J, Özmen S, El-Aty AMA. Toward personalized cancer management: Role of precision nutrition–diet interventions. Journal of Functional Foods. 2024; 123: 106584.

[2] Natarajan SR, Krishnamoorthy R, Alshuniaber MA, Al-Anazi KM, Farah MA, Rajagopal P, Palanisamy CP, Veeraraghavan VP, Jayaraman S. Identification of FOXM1 as a novel protein biomarker and therapeutic target for colorectal cancer progression: Evidence from immune infiltration and bioinformatic analyses. International Journal of Biological Macromolecules. 282 (Part 4): 137201.
[3] Rajendran MS, Jayaraman S, Khan JM, Jasmine S, Prabhakaran RK, Raju MV, Chandrasekaran MK, Ahalliya RM, Kannappan P, Palanisamy CP, Kanniappan GV. Investigating the colon toxicity and carcinogenic role of monosodium glutamate compared with Dimethylhydrazine in male Wistar rats: Exploring the link to childhood colon cancer risk. Journal of King Saud University - Science. 2024; 36(11): 103507.
[4] Kumarasamy RV, Natarajan P, Umapathy VR, Roy JR, Rab SO, Saeed M, Panagal M, Mironescu M, Srinivasan GP, Palanisamy CP. Clinical Applications and Therapeutic Potentials of Advanced Nanoparticles: A Comprehensive Review on Completed Human Clinical Trials. Frontiers in Nanotechnology. 2024; 6:1479993.
[5] Jin W, Pei JJ, Roy JR, Jayaraman S, Ahalliya RM, Kanniappan GV, Mironescu M, Palanisamy CP. Comprehensive review on single-cell RNA sequencing: A new frontier in Alzheimer's disease research. Ageing Research Reviews. 2024; 274: 102454.
[6] Pei J, Palanisamy CP, Jayaraman S, Natarajan PM, Umapathy VR, Roy JR, Panagal M, Jayaraman S. Curcumin-loaded polymeric nanomaterials as a novel therapeutic strategy for Alzheimer's disease: A comprehensive review. Ageing Research Reviews. 2024; 99: 102393.
[7] Pei J, Palanisamy CP, Jayaraman S, Natarajan PM, Umapathy VR, Roy JR, Thalamati D, Ahalliya RM, Kanniappan GV, Mironescu M. A comprehensive review on starch-based Sustainable Edible Films Loaded with Bioactive Components for Food Packaging. International Journal of Biological macromolecules. 2024; 274 (Part-1): 133332.
[8] Palanisamy CP, poompradub S, Sansanaphongpricha K, Subramani K, Sonsudin F. Increased expression levels of PDGF and VEGF magnify the wound healing potential facilitated by biogenic synthesis of silver nanoparticles. Nano-Structures & Nano-Objects. 2024; 39: 101236.
[9] Pei J, Palanisamy CP, Jayaraman S, Natarajan PM, Umapathy VR, Roy JR, Thalamati D, Ahalliya RM, Kanniappan GV, Mironescu M. Proteomics Profiling of Extracellular Vesicle for Identification of Potential Biomarkers in Alzheimer's Disease: A Comprehensive Review. Ageing Research Reviews. 2024; 99: 102359.
[10] Xi J, Wang T, Xian P, Liu X, Du M, Yang H, Palanisamy CP, Lin W, Long Q. Proteomic insights uncover enhanced neurotherapeutic potential in conditioned mesenchymal stem cell-derived extracellular vesicles. Extracellular Vesicle. 2024; 3: 100037.
[11] Pei J, Natarajan PM, Umapathy VR, Swamikannu B, Sivaraman NM, Krishnasamy L, Palanisamy CP. Advancements in the synthesis and functionalization of zinc oxide-based nanomaterials for enhanced oral cancer therapy. Molecules. 2024; 29(11): 2706.
[12] Gatasheh MK, Natarajan SR, Krishnamoorthy R, Alsulami TS, Rajagopal P, Palanisamy CP, Veeraraghavan VP, Jayaraman S. Molecular analysis to identify novel potential biomarkers as drug targets in colorectal cancer therapy: an integrated bioinformatics analysis. Molecular and Cellular Oncology. 2024; 11(1): 2326699.
[13] Pei J, Yan Y, Jayaraman S, Rajagopal P, Natarajan PM, Umapathy VR, Gopathy S, Roy JR, Sadagopan CS, Thalamati D, Palanisamy CP, Mironescu M. A review on advancements in the application of starch-based nanomaterials in biomedicine: Precision drug delivery and cancer therapy. International Journal of Biological Macromolecules. 2024; 130746.
[14] Pei JJ, Yan Y, Palanisamy CP, Jayaraman S, Natarajan PM, Umapathy VR, Gopathy S, Roy JR, Sadagopan JC, Thalamati D, Mironescu M. Materials-based drug delivery approaches: Recent advances and future perspectives. Green Processing and Synthesis. 2024; 13: 20230094.
[15] Pei JJ, Deng W, Liu Y, Guo Y, Chen J, Abdu H, Khan MR, Palanisamy CP, El-Aty AM. A Comprehensive Review of Cornus officinalis: Health Benefits, Phytochemistry, and Pharmacological Effects for Functional Drug and Food Development. Frontiers in Nutrition. 2023; 10: 1309963.
[16] Alugoju P, Palanisamy CP, Anthikapalli NVA, Jayaraman S, Prasanskulab A, Chuchawankul S, Dyavaiah M, Tencomnao T. Exploring the anti-aging potential of natural products and plant extracts in budding yeast Saccharomyces cerevisiae: A review. F1000Research. 2023; 12: 1265.
[17] Lavanya M, Krishnamoorthy R, Alshuniaber MA, Manoharadas S, Palanisamy CP, Veeraraghavan VP, Jayaraman S, Rajagopal P, Padmini R. Formulation, characterization and evaluation of gelatin-syringic acid/zinc oxide nanocomposite for its effective anticancer, antioxidant and anti-inflammatory activities. Journal of King Saud University-Science. 2023; 35: 102909.
[18] Palanisamy CP, Poompradub S, Sansanaphongpricha K, Jayaraman S, Subramani K, Sonsudin F. Biosynthesis of silver nanoparticles (AgNPs) using ethanolic extract of Nigella sativa (L.) seeds promotes wound healing via PDGF and VEGF signalling pathways activation. Biocatalysis and Agricultural Biotechnology. 2023; 54: 102970.
[19] Prasad M, Jayaraman S, Natarajan SR, Veeraraghavan VP, Krishnamoorthy R, Gatasheh MK, Palanisamy CP, Elrobh M. Piperine modulates IR/Akt/GLUT4 pathways to mitigate insulin resistance: Evidence from animal and computational studies. International Journal of Biological Macromolecules. 2023; 253: 127242.

[20] Palanisamy CP, Pei JJ, Phaniendra A, Venkata AAN, Jayaraman S, Veeraragahavan VP, Sridevi G, Roy JR, Janaki CS, Thalamati D, Mironescu M, Luo Q, Chai Y, Long Q. New Strategy of Neurodegenerative Disease Treatment with Extracellular Vesicles (EVs) Derived from Mesenchymal Stem Cells (MSCs). *Theranostics*. 2023; 13(12):4138-4165. doi:10.7150/thno.83066.
[21] Palanisamy CP, Phaniendra A, Jayaraman S, Poompradub S. *Nigella sativa* L. seed extracts promotes wound healing progress by activating VEGF and PDGF signalling pathways: *An in vitro* and *in silico* study. *F1000 Research*. 2023; 12: 436.
[22] Pei JJ, Palanisamy CP, Phaniendra A, Venkata AAN, Natarajan PM, Umapathy VR, Swamikannu B, Jayaraman S, Rajagopal P, Poompradub S. A comprehensive review on bio-based materials for chronic diabetic wounds. *Molecules*. 2022; 28(2), 604.
[23] Natarajan PM, Umapathy VR, Murali A, Swamikannu B. (2022). Computational Simulations of Identified marine-derived Natural Bioactive Compounds As Potential Inhibitors of Oral Cancer. Future Science OA. 2022; 8(3).
[24] Natarajan PM, Umapathy VR. Role of transcriptomics in the study of oral cancer. Frontiers in Oral Health. 2025; 6:1524364.
[25] Vidhyarekha U, Natarajan PM, Bhuminathan S, Sabarinathan J, Suba R, Vijayalakshmi P. Role of artificial intelligence in Oral Cancer. Advances in Public Health. 2024. 2024: 3664408.
[26] Ganesan A, Kumar NG, Natarajan PM, Gauthaman J. Automated classification of elongated styloid processes using deep learning models-an artificial intelligence diagnostics. Frontiers in Oral Health. 2025; 5: 1424840.
[27] Umapathy VR, Natarajan PM, Swamikannu B. Regenerative Strategies in Dentistry: Harnessing Stem Cells, Biomaterials and Bioactive Materials for Tissue Repair. Biomolecules. 2025; 15: 546.
[28] Natarajan PM. Dental Bioinformnatics-Current Scope and Future perspectives. Research Journal of Pharmacy and Technology. 2022;15(5):2351-6.
[29] Ganesan A, Kumar NG, Natarajan PM. Solanum trilobatum leaf extract-derived silver nanoparticles downregulate the PI3K/AKT/mTOR signaling pathway and attenuate oral squamous cell carcinoma cell proliferation. Journal of Herbmed Pharmacology. 2024; 13(2): 300-307.
[30] Perumal MKK, Renuka RR, Subbiah SK, Natarajan PM. Artificial intelligence-driven clinical decision support systems for early detection and precision therapy in oral cancer: a mini review. Frontiers in Oral Health. 2025; 6: 1592428.
[31] Ramesh E, Ganesan A, Lakshmi KC, Natarajan PM. Artificial intelligence-based diagnosis of oral leukoplakia using deep convolutional neural networks Xception and MobileNet-v2. Frontiers in Oral Health. 2025; 6: 1414524.
[32] Ganesan A, Kumar NG, Natarajan PM. Anticancer activity of silver nanoparticles synthesized from aqueous leaf extract of Solanum trilobatum (Purple fruit pea eggplant) on human oral cancer cells. Journal of Herbmed Pharmacololgy. 2024; 13(2): 260-268.
[33] Natarajan PM, Swamikannu B, Sivaraman NM, Stylin AGSQ. Prevention of Oral Cancer: A Comprehensive Guide. Journal of Pharmacy and Bioallied Sciences. 2024; 16(5): S4239-S4241.
[34] Jayaraman S, Eswaran A, Rajagopal P, Palanisamy CP, Veerakumar P, Veeraraghavan VP, Sirasanagandla SR. Neuroendocrine-associated epigenetic factors in cellular senescence: mechanisms and therapeutic implications. Biogerontology. 2026; 27(2): 64.
[35] Ponnusamy B, Rajagopal P, Palanisamy CP, Veeraraghavan VP, Jayaraman S. Mechanistic Exploration of the anticancer activity of Justicia adhatoda Plant Leaf Ethanolic Extract against Colon Cancer Cells: An in silico and in vitro Approach. Asian Pacific Journal of Cancer Prevention. 2026; 27(3): 1069-1080.
[36] Pei J, Saran VS, Sivaramakrishnan R, Kanniappan GV, Pandurangan V, Jayaraman S, Dhayalan VK, Mironescu M, Mironescu ID, Palanisamy CP. Ultrasonic-assisted, Sargassum ilicifolium (brown marine macroalgae)-mediated biogenic synthesis of CuO nanoparticles incorporated in starch/PVA electrospun nanoscaffolds: In vitro safety and antioxidant efficacy assessment. Bioorganic Chemistry. 2026; 173: 109679.
[37] Raj MAPA, Subramaniyam S, Kanniappan GV, Jayaraman S, Palanisamy CP. Sustainable fabrication of starch/PVA/CuO electrospun nanoscaffolds from Turbinaria ornata (marine macroalgae) extract: Physicochemical characterization and antidiabetic evaluation. Kuwait Journal of Science. 2026; 53(2): 100545.
[38] Pei J, Ganesh NS, Subramaniyam S, Sivaramakrishnan R, Kanniappan GV, Jayaraman S, Palanisamy CP. Sustainable fabrication of starch/PVA/CuO electrospun nanoscaffolds from Padina tetrastromatica (Brown macroalgae) extract: Physicochemical characterization and antidiabetic assessment. Sustainable Chemistry One World. 2026; 9: 100195.
[39] Sakthiraj A, Sivaramakrishnan R, Subramaniyam S, Kanniappan GV, Pandurangan V, Jayaraman S, Dhayalan VK, Mironescu M, Mironescu ID, Palanisamy CP. Starch/PVA electrospun nanoscaffolds loaded with ultrasonic-assisted green-synthesis of CuO nanoparticles from marine macroalgae (Gracilaria corticata) extract: Cytotoxicity and antioxidant analysis. Chemical Physics Impact. 2026; 12: 101018.
[40] Raju M, Chandrasekaran MK, Loganathan L, Ahalliya RM, Mironescu M, Mironescu ID, Palanisamy CP, Kanniappan GV. Lipid remodeling and ferroptosis in phosphatidylcholine-mediated tumor–stroma crosstalk. Frontiers in Molecular Biosciences. 2026; 13: 1742305.

[41] Kunamalla R, Panagal M, Palanisamy CP. Biogenic synthesis and fabrication of starch/PVA/CuO electrospun nanoscaffolds from Sargassum ilicifolium (brown marine macroalgae) extract for anticancer activity on HT-29 and MCF-7 cancer cells. Biocatalysis and Agricultural Biotechnology. 2026; 72: 103923.
[42] Pei J, Govindaraj H, Sivaramakrishnan R, Kanniappan GV, Pandurangan V, Dhayalan VK, Mironescu M, Mironescu ID, Jayaraman S, Palanisamy PC. Sustainable fabrication of biopolymer-based (starch/PVA) nanoscaffolds loaded with green-synthesized CuO nanoparticles from Sargassum wightii (marine macroalgae): Cytocompatibility and antioxidant activity. Biomaterials Advances. 2026; 182: 214660.
[43] Pei J, Perumal NC, Meng P, Long Q, Palanisamy CP. Extracellular vesicle-based biosensors for Alzheimer's disease: A new frontier in precision diagnostics. Ageing Research Reviews. 2026; 113: 102904.
[44] Shree P, Sivaramakrishnan R, Kanniappan GV, Pandurangan V, Jayaraman S, Dhayalan VK, Mironescu M, Mironescu ID, Palanisamy CP. Antioxidant and biocompatible CuO-starch/PVA nanoscaffolds via ultrasonic green synthesis using Turbinaria conoides (brown marine macroalgae). Medicine in Drug Discovery. 2025; 28: 100238.
[45] Gong J, Lin J, Guan T, Pei J, Palanisamy CP, El-AtyFrom AMA. selenium tolerance to nanoplastic antagonism: Comprehensive characterization of L. casei SNUT1 and its extracellular vesicle–nanoselenium complex. Food Bioscience. 2025; 74: 107749.
[46] Poochi SP, Sundarraj R, Raju MV, Chandrasekaran MK, Ahalliya RM, Palanisamy CP, Kanniappan GV, Kondapavuluri BK, Thiruvengadam M. Harnessing Nature: Computational and Experimental Insights Into *Ipomoea obscura* Metabolites for Bladder Cancer Therapy. Chemistry and Biodiversity. 2025; 0: e00909.
[47] Dugganaboyana GK, Kannankumar MKG, Shivaramakrishna S, Raju MV, Chandrasekaran MK, Ahalliya RM, Panneerselvam N, Palanisamy CP, Kanniappan GV. Phytochemical insights, antioxidant activity and therapeutic potential of Cassia senna against prostate cancer in Wistar albino rats. Discover Applied Sciences. 2025; 7:1206.
[48] Natarajan SR, Krishnamoorthy R, Alshuniaber MA, Gatasheh MK, Rajagopal P, Veeraraghavan VP, Palanisamy CP, Jayaraman S. KDM1A Facilitates Oncogenic Potential in Colorectal Cancer Progression Through the Activation of AXIN/GSK3β/β-Catenin Signaling Pathways: Evidence From Integrated Transcriptomics and In Vitro Studies. The Journal of Gene Medicine. 2025; 27(11): e70053.
[49] Guan T, Gong J, Lin J, Palanisamy CP, Jinjin Pei J, El-Aty AMA. Machine learning-driven multimodal optimization of selenium biotransformation and flavor profiling in fermented apple–Yacon functional beverages. Innovative Food Science & Emerging Technologies. 2025; 105: 104198.
[50] Natarajan SR, Krishnamoorthy R, Alshuniaber MA, Alsulami TS, Gatasheh MK, Rajagopal P, Palanisamy CP, Govindan R, Veeraraghavan VP, Jayaraman S. ABCE1 facilitates tumour progression via aerobic glycolysis and inhibits cell death in human colorectal cancer cells through the p53 signalling pathway. Scientific Reports. 2025; 15: 24674.
[51] Huang Y, Guo H, Liu Y, Jin W, Palanisamy CP, Pei J, Oz F, El-Aty AMA. Effects of Natural Polysaccharides on the Gut Microbiota Related to Human Metabolic Health. Molecular Nutrition & Food Research. 2025; 69:e202400792.
[52] Poornima K, Meenakshi K.C, Manikandan V.R, Shankari G, Prabhu D, Rathi M.A, Palanisamy CP, Balaji R, Gopalakrishnan V.K. Exploring the anticancer potential of Jerantinine A from *Tabernaemontana coronaria* against prostate, breast, and ovarian cancers: A computational approach. *Journal of Complementary and Integrative Medicine*, 2025 22(2): 363–372.
[53] Palanisamy CP, Poompradub S, Sansanaphongpricha K, Jayaraman S, Subramani K. Faridah Sonsudin gGreen synthesis of Nigella sativa-mediated silver nanoparticles for enhanced antibacterial activity and wound healing: Mechanistic insights and biomedical applications. Environmental Nanotechnology, Monitoring & Management. 2025; 24: 101085.
[54] Surendran N, Raju MV, Chandrasekaran MK, Ahalliya RM, Palanisamy CP, Chandrasekaran G, Kanniappan GV. Physicochemical characterization of starch from Maranta arundinacea L.(arrowroot) rhizomes and its inhibition of COX-2: In vivo validation. Bioactive Carbohydrates and Dietary Fibre. 2025; 33: 100465.
[55] Kannappan P, Chandrasekaran MK, Raju MV, Gopalakrishnan S, Dhamodharan P, Ahalliya RM, Palanisamy CP, Raju B, Kanniappan GV. Exploring the anticancer potential of Jerantinine A from Tabernaemontana coronaria against prostate, breast, and ovarian cancers: a computational approach. Journal of Complementary and Integrative Medicine. 2025; 22(02): 363-372.
[56] Pei J, Kumarasamy RV, Jayaraman S, Kanniappan GV, Long Q, Palanisamy CP. Quercetin-functionalized nanomaterials: Innovative therapeutic avenues for Alzheimer's disease management. Ageing Research Reviews. 2025; 104: 102665.
[57] Jayaraman S, Prasad M, Natarajan SR, Krishnamoorthy R, Alshuniaber MA, Gatasheh MK, Veeraraghavan VP, Rajagopal P, Palanisamy CP. Molecular mechanisms underlying the effects of beta-sitosterol on TGF-β1/Nrf2/SIRT1/p53-mediated signaling in the kidney of a high-fat diet and sucrose-induced type-2 diabetic rat. Chemico-Biological Interactions. 2025; 411: 111443.
[58] Umapathy V, Dhanavel A, Kesavan R, Natarajan PM, Bhuminathan S, Vijayalakshmi P. Anticancer Potential of the Principal Constituent of Piper nigrum, Piperine: A Comprehensive Review. Cureus. 2024; 16(2): e54425.

[59] Umapathy VR, Swamikannu B, Natarajan PM, Devi R, Nandini MS, Vimalarani, Vijayalakshmi P. In Silico Molecular Docking of Ocimum sanctum Phytochemicals: Targeting Key Biomarkers in Oral Cancer. Journal of Pharmacy and Bioallied Sciences. 2024; 16(5): S4792-S4799.
[60] Natarajan PM, Bhuminathan S, Rajan R, Bindu K, Loganathan K, Veerakumar R. The Crucial Role of Smoking Cessation in Preventing Oral Cancer. Journal of Pharmacy and Bioallied Sciences. 2024; 16(5): S4245-S4247.
[61] Swamikannu B, Umapathy VR, Natarajan PM, Nandini MS, Stylin AGSQ, Vimalarani V, Rajinikanth S. Unlocking the Therapeutic Benefits of Artemisia Annua: A Comprehensive Overview of its Medicinal Properties. Journal of Pharmacy and Bioallied Sciences. 2024; 16(5): S4248-S4253.
[62] Natarajan PM. Computational Studies on Recent Congeners of Fluoroquinolones and Nitroimidazoles for Their Use in Periodontal Therapy. Journal of Pharmacy and Bioallied Sciences. 2024; 16(5): S4731-S4740.
[63] Yadalam PK, Arumuganainar D, Natarajan PM, Ardila CM. Artificial intelligence-powered prediction of AIM-2 inflammasome sequences using transformers and graph attention networks in periodontal inflammation. Scientific Reports. 2025; 15: 8733.
[64] Yadalam PK, Chatterjee S, Natarajan PM, Ardila CM. Comparison of light gradient boosting and logistic r egression for interactomic hub genes in Porphyromonas gingivalis and Fusobacterium nucleatum-induced periodontitis with Alzheimer's disease. Frontiers in Oral Health. 2025; 6:1463458.
[65] Natarajan PM, Bhuminathan S, Leela B, Bindu K, Loganathan K, Ramachandran V. Smoking and its Role in Oral Cancer. Journal of Pharmacy and Bioallied Sciences 16(5): S4242-S4244.
[66] Yadalam PK, Natarajan PM, Ardila CM. Variational graph autoencoder for reconstructed transcriptomic data associated with NLRP3 mediated pyroptosis in periodontitis. Scientific Reports. 2025; 15: 1962.
[67] Manimaran D, Elangovan N, Mani P, Subramanian K, Ali D, Alarifi S, Palanisamy CP, Zhang H, Rangasamy K, Palanisamy V, Mani R, Govarthanan K, Aruni W, Shanmugam R, Srinivasan GP, Kalirajan A. Isolongifolene-loaded chitosan nanoparticles synthesis and characterization for cancer treatment. Scientific Reports. 2022; 12:19250.
[68] Palanisamy CP, Cui B, Zhang H, Gunasekaran VP, Ariyo A, Jayaraman S, Veeraraghavan V, Rajagopal P. A critical review on starch-based electrospun nanofibrous scaffolds for wound healing application. International Journal of Biological Macromolecules. 2022; 222 (Part: B): 1852-1860.
[69] Pei J, Umapathy VR, Vengadassalapathy S, Hussain SFJ, Rajagopal P, Jayaraman S*, Veeraraghavan VP, Palanisamy CP*, Gopinath K*. A Review of the Potential Conse-quences of Pearl Millet (Pennisetum glaucum) for Diabetes Mellitus and Other Biomedical Applications. Nutrients. 2022; 14(14):2932
[70] Monisha P, Ponnulakshmi R, Nalini D, Vishnu P V, Palanisamy CP, Cui B, Shankargouda P, Selvaraj J. A comprehensive review on high fat diet-induced diabetes mellitus: An epigenetic view. The Journal of Nutritional Biochemistry. 2022; 2022: 109037.
[71] Monisha P, Selvaraj J, Mohamed AE, Mohamed E, Mosaab AEA, Vishnu PV, Srinivasan V, Vidhya RU, Shazia FJH, Kalaiselvi K, Durairaj S, Palanisamy CP, Surapaneni K M, Ponnulakshmi R. A Comprehensive review on therapeutic perspectives of phytosterols in insulin resistance: A mechanistic approach. Molecules. 2022; 27(5): 1595.
[72] Kannayiram K, Umapathy VR, Chamundeswari Y, Fathima JH, Govindan R, Palanisamy CP, Veeraraghavan VP, Jayaraman S, Rajagopal P. Molecular docking analysis of flavonoids with aldose reductase. Bioinformation. 2022; 18(3): 80–83.
[73] UV Rekha, Varadhachariyar R, Rajagopal P, Priya PH, Fathima JHS, Govindan R, Palanisamy CP, Veeraraghavan VP, Jayaraman S. Molecular docking analysis of bioactive compounds from Plectranthus amboinicus with glucokinase. Bioinformation. 2022; 18(3): 261–264.
[74] Umapathy VR, Rajagopal P, Varadhachariyar R, Priya PH, Fathima JHS, Govindan R, Palanisamy CP, Brindha KBA, Veeraraghavan VP, Jayaraman S. Molecular docking analysis of bioactive compounds from Cissampelos pareira with PPAR gamma. Bioinformation. 2022; 18(3): 265-268.
[75] Rajagopal P, Umapathy VR, Sandhya P, Fathima JH, Govindan R, Palanisamy CP, Veeraraghavan VP, Jayaraman S. Molecular docking analysis of metformin analogues with GSK-3β. Bioinformation. 2022; 18(3): 269-272.
[76] Adeniran LA, Palanisamy CP, Ashafa AOT. Chemical profiling, in vitro antioxidant and antidiabetic assessment of flavonoids from the ethanol extract of Hermannia geniculata root. Sokoto Journal of Veterinary Sciences. 2021; 19(1): 1-13.
[77] Sundaram S, Palanisamy CP, Subban R, Palanirajan A, Piramanayagam S, Eswaran M, Krishna CK, Kanniappan VG. 1-Pentacosanol Isolated from Stem Ethanolic Extract of Cayratia trifolia (L.) is A Potential Target for Prostate Cancer-In SILICO Approach. Jordan Journal of Biological Sciences. 2021; 14 (2): 359-365.
[78] Raj SS, Palanisamy CP, Mani P. Antioxidant, antimicrobial and cytotoxicity of n-hexane extract from Mollugo nudicaulis Lam. Bioinformation. 2021; 17 (5), 573-582.
[79] Palanisamy CP, Cui B, Zhang H, Panagal M, Paramasivam S, Chinnaiyan U, Jeyaraman S, Murugesan K, Rostagno M, Sekar V, Natarajan SP. Anti-ovarian cancer potential of phytocompound and extract from South African medicinal plants and their role in the development of chemotherapeutic agents. American Journal of Cancer Research. 2021; 11(5):1828-1844.

[80] Palanisamy CP, Pethanan S, Vincent GG, Murugesan K, Ramachandran A, Sivanandam R, Panagal M. Chemotherapeutic potential of Cayratia trifolia L nhexane extract on A2780 cells. Bioinformation. 2021; 17(8): 710–714.
[81] Palanisamy CP, Fathima JHS, Sekar R, Rajagopal P, Jeyaraman S. MTT assay based inhibition analysis of A2780 cells proliferation using Mollugo nudicaulis Lam. extract with CXCR4 and HER2 expression. Bioinformation. 2021; 17(7): 705–709.
[82] Jayaraman S, Devarajan N, Rajagopal P, Babu S, Ganesan SK, Veeraraghavan VP, Palanisamy CP, Cui B, Periyasamy V, Chandrasekar K. β-Sitosterol Circumvents Obesity Induced Inflammation and Insulin Resistance by down-Regulating IKKβ/NF-κB and JNK Signaling Pathway in Adipocytes of Type 2 Diabetic Rats. Molecules. 2021; 26: 2101.
[83] Bhuvaneswari M, Palanisamy CP, Mani P. Antioxidant, antimicrobial and cytotoxicity potential of n-hexane extract of Cayratia trifolia L. Bioinformation. 2021; 17(3): 452-459.